

Synthesis and Characterization of a High-Symmetry Ferrous Polypyridyl Complex: Approaching the $^5T_2/{}^3T_1$ Crossing Point for Fe^{II}

Lindsey L. Jamula, Allison M. Brown, Dong Guo, and James K. McCusker*

Department of Chemistry, Michigan State University, 578 South Shaw Lane, East Lansing, Michigan 48824, United States

Supporting Information

ABSTRACT: Electronic structure theory predicts that, depending on the strength of the ligand field, either the quintet (5T_2) or triplet (3T_1) term states can be stabilized as the lowest-energy ligand-field excited state of low-spin octahedral d^6 transition-metal complexes. The 3T_1 state is anticipated for second- and third-row metal complexes and has been established for certain first-row compounds such as $[Co(CN)_6]^{3-}$, but in the case of the widely studied Fe^{II} ion, only the 5T_2 state has ever been documented. Herein we report that 2,6-bis(2-carboxypyridyl)pyridine (dcpp), when bound to Fe^{II} , presents a sufficiently strong ligand field to Fe^{II} such that the $^5T_2/{}^3T_1$ crossing point of the d^6 configuration is approached if not exceeded. The electrochemical and photophysical properties of $[Fe(dcpp)]^{2+}$, in addition to being of fundamental interest, may also have important implications for solar energy conversion strategies that seek to utilize earth-abundant components.

Ligand-field theory represents one of the conceptual pillars of inorganic chemistry. Indeed, the metal-based, so-called “d-d” electronic states of such compounds were predicted nearly 60 years ago.^{1,2} In the case of a six-coordinate d^6 species, ligands presenting a weak-field potential lead to an adherence to Hund’s rule and a 5T_2 term as the compound’s ground state; as the ligand-field strength is increased, the low-spin 1A_1 term is stabilized, eventually becoming the ground state once the t_{2g} /e_g orbital splitting exceeds the spin-pairing energy (the “spin-crossover” point).^{3,4} With the notable exception of the recent report by Wärnmark and co-workers,⁵ these ligand-field states effectively define the photophysics of iron(II) complexes.^{6–9}

Given a sufficiently strong ligand field, the lowest-energy triplet excited state (3T_1) eventually drops below the 5T_2 term to become the lowest-energy ligand-field excited state of the system. This is uniformly the case in the second and third transition series; with the exception of $[Co(CN)_6]^{3-}$, whose emission near 800 nm has been assigned as a ${}^3T_1 \rightarrow {}^1A_1$ transition,¹⁰ no corresponding example of this phenomenon has been definitively established for a first-row d^6 metal complex.¹¹ With this Communication, we describe the first example of a new class of iron(II) polypyridyl chromophores for which this crossing point is within reach. Specifically, we report that the previously known ligand 2,6-bis(2-carboxypyridyl)pyridine¹² (which we abbreviate as dcpp) forms a bisadduct with Fe^{II} . The resulting compound, $[Fe(dcpp)]_2(PF_6)_2$, has been characterized by single-crystal X-ray crystallography to reveal a near-perfect octahedral primary coordination sphere. This geometry, coupled with the

low-energy nature of the ligand’s π^* orbitals, results in a significant stabilization of the t_{2g} orbitals of the Fe^{II} center and photoinduced dynamics consistent with a significant perturbation of the compound’s low-lying excited electronic structure.

Inspired by the work of Schramm and co-workers, who prepared the corresponding ruthenium(II) complex of the dcpp ligand,¹³ we attempted unsuccessfully to prepare the iron(II) analogue by a similar route. The formation of Fe^{III} -containing products in the reaction mixture suggested that, in contrast to the Schramm reaction with Ru^{II} , oxidation of Fe^{II} occurs more readily than oxidation of the ligated, reduced precursor of dcpp, 2,6-bis(2-methylene-pyridyl)pyridine (dmpp). The dcpp ligand was therefore prepared directly according to literature methods.¹² $[Fe(dcpp)](PF_6)_2$ was then synthesized by transferring a $MeOH/H_2O$ solution of $FeCl_2 \cdot 2H_2O$ to that of dcpp using Schlenk techniques. The reaction mixture was stirred for 19 h at room temperature under nitrogen, after which the product was obtained in 54% yield by precipitation with NH_4PF_6 and subsequent purification.

$[Fe(dcpp)](PF_6)_2$ crystallizes in the orthorhombic space group $Pbcn$ and is situated on the crystallographic inversion center, making only half of the molecule unique. Each Fe^{II} ion is coordinated by two tridentate ligands, forming a six-coordinate complex (Figure 1). Similar to the reported structure of $[Ru(dcpp)]^{2+}$,¹³ the coordination geometry of the Fe^{II} center in $[Fe(dcpp)]^{2+}$ corresponds to a nearly perfect octahedron with cis and trans bond angles deviating only slightly from the ideal values of 90° and 180° ($90.35 \pm 0.55^\circ$ and $178.3 \pm 0.7^\circ$, respectively). This is in stark contrast to the closely related $[Fe(terpy)]^{2+}$ complex (where terpy is 2,2':6',2''-terpyridine), whose bond angles vary in the ranges of 79.8 – 100.5° and 161.0 – 178.7° for cis and trans, respectively.¹⁵ Even the tris-bidentate complex $[Fe(bpy)]_3^{2+}$ (where bpy is 2,2'-bipyridine) exhibits a more significant deviation from octahedral geometry (81.8 – 94.3° and 174.6°) than that seen for $[Fe(dcpp)]^{2+}$.¹⁶ These differences are most likely associated with the relative rigidity of the bpy and terpy ligands coupled with the five-membered ring nature of the chelate, whereas the dcpp ligand can adopt a less sterically constrained configuration around the metal center because of the presence of the carbonyl groups that bridge between the pyridyl rings.¹³ The Fe –N bond distances in $[Fe(dcpp)]^{2+}$ are unremarkable for low-spin nitrogen-coordinated Fe^{II} at $1.98 \pm 0.02 \text{ \AA}$; this is comparable to both $[Fe(bpy)]_3^{2+}$ (1.97 \AA) and $[Fe(terpy)]^{2+}$ (1.89 – 2.00 \AA).

Received: September 23, 2013

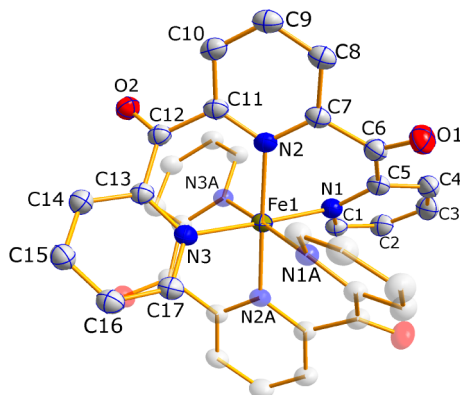


Figure 1. ORTEP drawing of the cation of $[\text{Fe}(\text{dcpp})_2](\text{PF}_6)_2$ obtained from single-crystal X-ray structure determination. Atoms are represented as 50% probability thermal ellipsoids. Hydrogen atoms and anions are omitted for clarity. Selected bond lengths (Å) and angles (deg): Fe1–N1 , 1.985(2); Fe1–N2 , 1.974(2); Fe1–N3 , 1.989(2); O2–C12 , 1.211(2); O1–C6 , 1.213(2); N2–Fe1–N1A , 90.48(7); N2–Fe1–N1 , 88.79(6); N2–Fe1–N3 , 88.87(6); N2–Fe1–N3A , 91.86(6); N1–Fe1–N1A , 90.61(9); N1–Fe1–N3A , 89.07(7); N3–Fe1–N3A , 91.35(9); N1–Fe1–N3 , 177.63(6); N2–Fe1–N2A , 178.96(8). Symmetry code A: $-x, y, -z + 1/2$.¹⁴

The dcpp ligand is twisted in a propeller-like arrangement that facilitates the creation of the octahedral coordination geometry. Interestingly, intramolecular interligand π – π -stacking interactions are found between each of the carbonyl groups of one dcpp ligand and a nearby peripheral pyridine ring of another dcpp ligand. The shortest interplanar atom–atom separations and dihedral angles are 2.87 Å (19.3°) and 2.84 Å (18.8°) for the stacked pairs, respectively, with center-to-center separations of these stacked pairs of 3.26 and 3.40 Å. Whether these π – π interactions are the result of or contributing to the compressed geometry is unclear.

The reason for the unusual blue color of $[\text{Fe}(\text{dcpp})_2](\text{PF}_6)_2$ is evident from the compound's electronic absorption spectrum (Figure S1 in the SI), where the $^1\text{A}_1 \rightarrow ^1\text{MLCT}$ absorption feature exhibits a maximum at 610 nm. The charge-transfer envelope for $[\text{Fe}(\text{dcpp})_2]^{2+}$ spans a broad range from 425 to 650 nm; the ca. 3500 cm⁻¹ separation between the maxima suggests that these features represent distinct electronic transitions as opposed to a vibronic structure of a single feature. Although the molar absorptivity of the MLCT maximum is smaller for $[\text{Fe}(\text{dcpp})_2]^{2+}$ than either $[\text{Fe}(\text{bpy})_3]^{2+}$ or $[\text{Fe}(\text{terpy})_2]^{2+}$, integrating the spectra across the entire charge-transfer envelope (14000–25000 cm⁻¹) indicates a slight increase in the visible absorption cross section of $[\text{Fe}(\text{dcpp})_2]^{2+}$ relative to the other two compounds. We anticipate that more details will emerge from ongoing time-dependent DFT calculations.

Electrochemical data for $[\text{Fe}(\text{dcpp})_2]^{2+}$ are listed in Table 1; a plot of the cyclic voltammogram is shown in Figure S2 in the SI. The first oxidation wave is observed at $E_{1/2} = 1.29$ V versus the ferrocene/ferrocenium and is assigned to the $\text{Fe}^{\text{II}}/\text{Fe}^{\text{III}}$ couple. This is ca. 600 mV more positive than the corresponding oxidations of $[\text{Fe}(\text{bpy})_3]^{2+}$ and $[\text{Fe}(\text{terpy})_2]^{2+}$ and indicates a significant degree of stabilization of the formally π -bonding t_2 orbitals in $[\text{Fe}(\text{dcpp})_2]^{2+}$ relative to these other compounds. We believe this is partly due to the coordination geometry described earlier, wherein the near-perfect octahedral symmetry of the primary coordination sphere enhances the directionality of the metal–ligand orbital overlap. A second, perhaps more significant, contributing factor is likely the low energy of the π^* orbital of

Table 1. Electrochemical Data for $[\text{Fe}(\text{dcpp})_2](\text{PF}_6)_2$, $[\text{Fe}(\text{bpy})_3](\text{PF}_6)_2$, and $[\text{Fe}(\text{terpy})_2](\text{PF}_6)_2$

compound	$E_{1/2}$ (V)	
	oxidation	reduction
$[\text{Fe}(\text{dcpp})_2]^{2+}$	1.29	-0.97
$[\text{Fe}(\text{bpy})_3]^{2+}$	0.66	-1.78
$[\text{Fe}(\text{terpy})_2]^{2+}$	0.71	-1.68

^aElectrochemical data were measured with a 0.1 M TBAPF₆ electrolyte in MeCN using Ag/AgNO₃ as a reference. The tabulated values represent the potentials externally referenced to Fc/Fc⁺. Potentials are estimated to be accurate to ± 0.02 V. Further details are available in the SI.

dcpp. The significant positive shift in the reduction potential of ligated dcpp relative to bpy and terpy has been attributed to the presence of the electron-withdrawing carbonyl groups in the dcpp backbone.¹³ This will result in a better energetic match with the filled d orbitals of the Fe^{II} center, which, in turn, will give rise to increased mixing and stabilization of the bonding t_2 set. Although we have no direct experimental information concerning the energy of the e^* (i.e., σ -antibonding) orbitals, the fairly typical Fe–N bond distance coupled with the symmetry of the primary coordination sphere suggests that the e^* orbitals in $[\text{Fe}(\text{dcpp})_2]^{2+}$ are either isoenergetic with or slightly more destabilized than what is found for the bpy- and terpy-based analogues. Our conclusion, therefore, is that $[\text{Fe}(\text{dcpp})_2]^{2+}$ is characterized by an increase in the ligand-field strength of ≥ 600 mV relative to both $[\text{Fe}(\text{bpy})_3]^{2+}$ and $[\text{Fe}(\text{terpy})_2]^{2+}$ due to the unique ligating properties of dcpp.

Photoexcitation of low-spin iron(II) polypyridyl complexes results in the rapid formation of the lowest-energy excited state of the system, whereupon the compound relaxes back to its ground state.^{6–9} The time constant for $^5\text{T}_2 \rightarrow ^1\text{A}_1$ relaxation in $[\text{Fe}(\text{bpy})_3]^{2+}$ is 0.96 ± 0.02 ns in a CH₃CN solution (Figure 2,

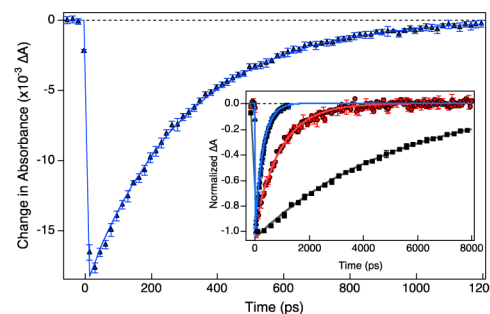


Figure 2. Time-resolved electronic absorption data for $[\text{Fe}(\text{bpy})_3](\text{PF}_6)_2$ (red, inset), $[\text{Fe}(\text{terpy})_2](\text{PF}_6)_2$ (black, inset), and $[\text{Fe}(\text{dcpp})_2](\text{PF}_6)_2$ (blue) in room temperature CH₃CN solutions following excitation near the maximum of each compound's $^1\text{A}_1 \rightarrow ^1\text{MLCT}$ visible absorption feature. The solid lines correspond to fits of the data to single-exponential kinetic models with time constants of 0.96 ± 0.02 , 5.35 ± 0.15 , and 0.28 ± 0.01 ns, respectively.

inset). Energetic considerations¹⁷ as well as variable-temperature time-resolved absorption measurements¹⁸ place the ground-state recovery dynamics of $[\text{Fe}(\text{bpy})_3]^{2+}$ at or near the barrierless region; $[\text{Fe}(\text{terpy})_2]^{2+}$ possesses a smaller $^1\text{A}_1/{}^5\text{T}_2$ energy gap than $[\text{Fe}(\text{bpy})_3]^{2+}$ and gives rise to a longer excited-state lifetime (Figure 2, inset). The significantly larger ligand-field splitting associated with $[\text{Fe}(\text{dcpp})_2]^{2+}$ should push the zero-point energy of its ${}^5\text{T}_2$ state past $[\text{Fe}(\text{bpy})_3]^{2+}$ into the inverted region,

resulting in an excited-state lifetime for $[\text{Fe}(\text{dcpp})_2]^{2+}$ more comparable to that of $[\text{Fe}(\text{terpy})_2]^{2+}$. However, the dynamics associated with ground-state recovery for $[\text{Fe}(\text{dcpp})_2]^{2+}$ are more than a factor of 3 *faster* than what is observed for $[\text{Fe}(\text{bpy})_3]^{2+}$ under identical experimental conditions (Figure 2). We also prepared and characterized $\text{Fe}(\text{bpy})_2(\text{CN})_2$, in which one of the bipyridyl ligands has been replaced by two cyano groups. This compound exhibits an excited-state lifetime in a room temperature CH_3CN solution of 630 ± 10 ps, shorter than that of $[\text{Fe}(\text{bpy})_3]^{2+}$ but still more than a factor of 2 longer than what we measure for $[\text{Fe}(\text{dcpp})_2]^{2+}$.

Two possible explanations immediately come to mind that could explain these observations: (1) the reorganization energy associated with $^5\text{T}_2 \rightarrow ^1\text{A}_1$ relaxation is significantly different for $[\text{Fe}(\text{dcpp})_2]^{2+}$ than what is being inferred for these other compounds or (2) different excited electronic states are involved in the relaxation dynamics. Variable-temperature time-resolved absorption measurements recently carried out in our laboratory have shown that the reorganization energy associated with $^5\text{T}_2 \rightarrow ^1\text{A}_1$ relaxation in the $[\text{Fe}(\text{tren}(\text{py})_{3-x}(6\text{-Me-py})_x)]^{2+}$ class of spin-crossover complexes is on the order of 1.0 eV.¹⁸ Considering the degree of stabilization of the t_2 -type orbitals in $[\text{Fe}(\text{dcpp})_2]^{2+}$, the value of λ for ground-state recovery would have to be significantly larger for $[\text{Fe}(\text{dcpp})_2]^{2+}$ in order to produce the kinetics shown in Figure 2. A second, more intriguing possibility is that the enhanced ligand-field strength of the dcpp ligand has pushed this system past the $^5\text{T}_2/{}^3\text{T}_1$ crossing point, thereby changing the nature of the lowest-energy excited state being sampled in the photophysical measurement. In this scenario, we would expect a smaller value for λ , given the difference in the electronic configuration [i.e., $(t_2)^5(e^*)^1$ for ${}^3\text{T}_1$ versus $(t_2)^4(e^*)^2$ for ${}^5\text{T}_2$], as well as an increase in the electronic coupling between the ground and excited states due to the reduction in the net spin change associated with the relaxation process.

The above discussion assumes that the relative positions of the excited-state potential energy surfaces are the main determining factors dictating the kinetics, which is clearly an oversimplification of the problem. A more extensive series of studies, including variable-temperature ultrafast time-resolved electronic absorption measurements, time-resolved X-ray absorption, and computational studies on this and related synthetic analogues that we have recently prepared,¹⁹ are currently underway in order to understand the dynamics of this system in greater detail.

Apart from the fundamental interest in this compound from the perspective of electronic structure theory, the physical and photophysical properties of what we view as the first member of a novel class of iron(II) complexes could pave the way for their use in certain applications. For example, the Fe^{III} form of $[\text{Fe}(\text{dcpp})_2]^{2+}$ is a reasonably strong oxidant, which if transiently generated could form the basis of a potent photoredox agent. In addition, the close energetic proximity of the lowest-energy charge-transfer and ligand-field excited states coupled with the compound's broad electronic absorption profile presents interesting opportunities for applications in various solar energy conversion schemes. Work along these lines is ongoing.

ASSOCIATED CONTENT

Supporting Information

General synthetic procedures, syntheses, and characterization of dcpp and $[\text{Fe}(\text{dcpp})_2](\text{PF}_6)_2$, details concerning steady-state and time-resolved measurements, and X-ray crystallography in CIF

format. This material is available free of charge via the Internet at <http://pubs.acs.org>.

AUTHOR INFORMATION

Corresponding Author

*E-mail: jkm@chemistry.msu.edu.

Notes

The authors declare no competing financial interest.

ACKNOWLEDGMENTS

The authors thank Jennifer Miller for acquiring the time-resolved electronic absorption data on $\text{Fe}(\text{bpy})_2(\text{CN})_2$. This work was supported by the Chemical Sciences, Geosciences, and Biosciences Division, Office of Basic Energy Science, Office of Science, U.S. Department of Energy, under Grant DE-FG02-01ER152.

REFERENCES

- (1) Tanabe, Y.; Sugano, S. *J. Phys. Soc. Jpn.* **1954**, 9, 766.
- (2) Shimura, Y.; Tsuchida, R. *Bull. Chem. Soc. Jpn.* **1955**, 28, 572.
- (3) Gutlich, P.; Goodwin, H. A. *Top. Curr. Chem.* **2004**, 233, 1.
- (4) Hauser, A. *Top. Curr. Chem.* **2004**, 234, 155.
- (5) Liu, Y.; Harlang, T.; Canton, S. E.; Chábera, P.; Suárez-Alcántara, K.; Fleckhaus, A.; Vithanage, D. A.; Göransson, E.; Corani, A.; Lomoth, R.; Sundström, V.; Wärnmark, K. *Chem. Commun.* **2013**, 49, 6412.
- (6) Monat, J. E.; McCusker, J. K. *J. Am. Chem. Soc.* **2000**, 122, 4092.
- (7) Smeigh, A. L.; Creelman, M.; Mathies, R. A.; McCusker, J. K. *J. Am. Chem. Soc.* **2008**, 130, 14105.
- (8) Cho, H.; Strader, M. L.; Hong, K.; Jamula, L.; Gullickson, E. M.; Kim, T. K.; de Groot, F. M. F.; McCusker, J. K.; Schoenlein, R. W.; Huse, N. *Faraday Discuss.* **2012**, 157, 463 and references cited therein.
- (9) Gawelda, W.; Pham, V. T.; van der Veen, R. M.; Grolimund, D.; Abela, R.; Chergui, M.; Bressler, C. *J. Chem. Phys.* **2009**, 130, 124520 and references cited therein.
- (10) Miskowski, V. M.; Gray, H. B.; Wilson, R.; Solomon, E. *Inorg. Chem.* **1979**, 18, 1410.
- (11) The energetics of the ${}^3\text{T}_1$ excited state of $[\text{Fe}(\text{CN})_6]^{4-}$ has been considered by other researchers, albeit from the perspective of excitation (as opposed to zero-point) energies. See, for example: (a) Alexander, J. J.; Gray, H. B. *J. Am. Chem. Soc.* **1968**, 90, 4260. (b) Pierloot, K.; Van Praet, E.; Vanquickenborne, L. G.; Roos, B. O. *J. Phys. Chem.* **1993**, 97, 12220.
- (12) (a) Goldsmith, C. R.; Stack, T. D. P. *Inorg. Chem.* **2006**, 45, 6048. (b) Abarca, B.; Ballesteros, R.; Elmasnaouy, M. *Tetrahedron* **1998**, 54, 15287.
- (13) Schramm, F.; Meded, V.; Fliegl, H.; Fink, K.; Fuhr, O.; Qu, Z.; Klopper, W.; Finn, S.; Keyes, T. E.; Ruben, M. *Inorg. Chem.* **2009**, 48, 5677.
- (14) Crystallographic data for $[\text{Fe}(\text{dcpp})_2](\text{PF}_6)_2$: $\text{C}_{34}\text{H}_{22}\text{F}_{12}\text{FeN}_5\text{O}_4\text{P}_2$ (924.37 g/mol), $T = 173$ (2) K, Mo $\text{K}\alpha$ radiation ($\lambda = 0.71073$ Å), orthorhombic, space group $Pb\bar{c}n$, $Z = 4$, $a = 14.5603(3)$ Å, $b = 15.4333(3)$ Å, $c = 15.0431(3)$ Å, $V = 3380.39(12)$ Å³, $\mu = 0.66$ mm⁻¹, $2\theta_{\text{max}} = 56.6^\circ$, $F_{000} = 1856$ and 21855 reflections measured, of which 4199 were independent and 3524 reflections with $I > 2\sigma(I)$, $R_{\text{int}} = 0.072$ and 267 parameters, $R1 = 0.047$, $wR2 = 0.125$, GOF = 1.05 ($R1 = \sum \|F_o - |F_c|\| / \sum |F_o|$; $wR2 = [\sum [w(F_o^2 - F_c^2)^2] / \{\sum [w(F_o^2)^2]\}]^{1/2}$).
- (15) (a) Oshio, H.; Spiering, H.; Ksenofontov, V.; Renz, F.; Gutlich, P. *Inorg. Chem.* **2001**, 40, 1143. (b) Baker, A. T.; Goodwin, H. A. *Aust. J. Chem.* **1985**, 38, 207.
- (16) Dick, S. Z. *Kristallogr.: New Cryst. Struct.* **1998**, 213, 356.
- (17) Sutin, N. *Acc. Chem. Res.* **1982**, 15, 275.
- (18) Brown, A. M.; Jamula, L. L.; McCusker, J. K., unpublished results.
- (19) Jamula, L. L. Ph.D. Dissertation, Michigan State University, East Lansing, MI, 2013.